HHS Public Access

Author manuscript

J Thorac Oncol. Author manuscript; available in PMC 2021 April 01.

Published in final edited form as:

J Thorac Oncol. 2020 April ; 15(4): 589–600. doi:10.1016/j.jtho.2019.12.112.

THREE-DIMENSIONAL HISTOLOGIC, IMMUNOHISTOCHEMICAL AND MULTIPLEX IMMUNOFLUORESCENCE ANALYSIS OF DYNAMIC VESSEL CO-OPTION OF SPREAD THROUGH AIR SPACES (STAS) IN LUNG ADENOCARCINOMA

Yukako Yagi, M.D.[1], **Rania G. Aly, M.D., Ph.D.**[1,2], **Kazuhiro Tabata, M.D., Ph.D.**[1,3], **Afsar Barlas, M.D.**[4], **Natasha Rekhtman, M.D. Ph.D.**[1], **Takashi Eguchi, M.D.**[5,6], **Joeseph Montecalvo, M.D.**[1,7], **Meera Hameed, M.D.**[1], **Katia Manova-Todorova, Ph.D.**[4], **Prasad S. Adusumilli, M.D.**[5,8], **William D. Travis, M.D.**[1]

[1]Dept of Pathology, Memorial Sloan Kettering Cancer Center, New York, NY

[2]Department of Pathology, Alexandria University, Alexandria, Egypt

[3]Dept of Pathology, Nagasaki University Hospital, Nagasaki, Japan

[4]Molecular Cytology, Core Facility, Memorial Sloan Kettering Cancer Center, New York, NY

[5]Thoracic Surgery Service, Memorial Sloan Kettering Cancer Center

[6]Division of Thoracic Surgery, Department of Surgery, Shinshu University, Matsumoto, Japan

[7]Dept of Pathology, Henry Ford Hospital, Detroit, MI

[8]Center for Cell Engineering, Memorial Sloan Kettering Cancer Center, New York, NY

Abstract

Background: Spread through air spaces (STAS) is a method of invasion in lung adenocarcinoma, associated with tumor recurrence and poor survival. The spatial orientation of STAS cells/clusters to the lung alveolar parenchyma is not known. The aim of this study was to utilize high resolution and high-quality three-dimensional (3D) reconstruction of images from immunohistochemistry (IHC) and multiplex immunofluorescence (IF) experiments to understand the spatial architecture of tumor cell clusters by STAS in the lung parenchyma.

Methods: Four lung adenocarcinomas: 3 micropapillary (MIP) predominant and 1 solid (SN) predominant adenocarcinoma subtypes, were investigated. A 3D reconstruction image was created from the formalin fixed paraffin-embedded (FFPE) blocks. 350 serial sections were obtained and stained with hematoxylin and eosin (H&E) (100 slides), IHC (200 slides), and multiplex IF (50

[1]Correspondence: Yukako Yagi, M.D. Dept of Pathology, Memorial Sloan Kettering Cancer Center 1275 York Ave New York, NY 10065 yagiy@mskcc.org Tel: 646-888-7470.

DISCLOSURES: None.

slides) with the following antibodies: CD31, collagen type 4, TTF-1 and E-Cadherin. Whole slide images (WSIs) were reconstructed into 3D images for evaluation.

Results: Serial 3D image analysis by H&E as well as IHC and IF showed the MIP clusters and SN nests of STAS focally attached to alveolar walls away from the main tumor.

Conclusion: Our 3-D reconstructions demonstrated STAS tumor cells can attach to alveolar walls rather than appearing free floating as seen on 2D sections. This suggests that tumor cells detach from the main tumor, migrate through air spaces and reattach to alveolar walls through vessel co-option allowing them to survive and grow. This may explain the higher recurrence rate and worse survival for STAS positive tumors undergoing limited resection compared to lobectomy.

Keywords

Spread through air spaces (STAS); co-option; survival; three-dimensional analysis; multiplex immunofluorescence

Introduction

Since the initial description in 2015[1, 2] there has been great interest in the study of spread through air spaces (STAS) in lung cancer with multiple worldwide investigative groups publishing data from over 3500 patients documenting its presence in 15–60% of lung adenocarcinomas and its strong correlation with recurrence and poor survival.[3–12] It is defined as the presence of tumor cells within the air spaces in the lung parenchyma beyond the edge of the main tumor.[2, 13] In lung adenocarcinoma, three patterns of STAS were identified: micropapillary (MIP), solid nests (SN) and single cells.[2, 13] Although initially described in lung adenocarcinoma, the prognostic significance has been demonstrated in all major histologic types of lung cancers investigated including squamous cell carcinoma,[14, 15] small cell carcinoma,[16] large cell neuroendocrine carcinoma,[16], atypical carcinoid[16] and pleomorphic carcinoma.[17]

The association between STAS and tumor recurrence as well as patient survival raises the question about the mechanisms by which these malignant cells, observed floating in the air spaces in two-dimensional (2D) conventional images, spread through the air spaces and how they survive. The spatial organization of STAS cells/clusters and their relationship to the lung alveolar parenchyma is not known. The concept of blood vessel co-option has been raised to explain how tumor cells use the host vessels for their survival, growth and metastasis. [18–21]

The development of the whole slide imaging (WSI) technology which involves the breakthrough computer based three-dimensional (3D) reconstruction and visualization of the histology images has opened a new era of pathology research and diagnosis. WSI technology allows for a high-resolution panoramic and detailed image of stained sections and the 3D reconstruction allows the observation of series of serial sections generating a detailed image, with high volume and high speed.[22] The development of the technology has progressed to include not only hematoxylin and eosin (H&E) stains, but also special immunohistochemical (IHC) and immunofluorescence (IF) stains.[23] These technical modifications, and their combination with the protein expression assessment and the

molecular analysis assays, make them useful for studying not only the detailed cellular morphology and the anatomic intercellular relationships but also the cell biology and function.

Since its development, the WSI based 3D has led to valuable insights in its application to digital and molecular pathology in lymphoma and glioblastoma.[22, 24, 25] In lung adenocarcinoma, the WSI based 3D imaging technology has previously been used to identify the presence of "tumor islands," which in retrospect represents an early recognition of STAS that was also associated with poor prognosis.[26, 27]

As the spatial relationship of STAS cells/clusters and the alveolar walls is not known and considering the limitation of the two-dimensional (2D) conventional image, we sought to study lung adenocarcinomas with STAS focusing on the relationship between STAS and the surrounding microenvironment, including the alveolar vasculature, by performing a detailed structural, immunohistochemical and immunofluorescence investigation using WSI.

Materials and methods:

I- Materials:

This study was approved by the Institutional Review Board at Memorial Sloan Kettering Cancer Center (MSKCC) # 17–062. The study includes a cohort of four lung adenocarcinoma specimens: three MIP predominant adenocarcinoma and one solid predominant adenocarcinoma. The four specimens were previously diagnosed as lung adenocarcinoma with STAS in the pathology department, MSKCC.

II- Methods:

A. Histological examination: The H&E slides of four lung adenocarcinoma tumors were retrieved and reviewed by 2 expert pathologists (R.G.A and W.D.T). The four cases were selected based on the tissue quality, the amount of STAS with different morphological subtypes. The H&E slides of all cases were reviewed to 1) assess the percentages of the different histological subtypes and to determine the predominant subtype, 2) to identify the presence of STAS, and 3) to determine the pattern of STAS. The slide review was done using Olympus BX51 microscope (Olympus, Tokyo, Japan). The histological subtyping and the identification of STAS were based on the 2015, WHO classification of lung cancer.[13] Part of the criteria used to diagnose STAS included our previously published approach to the differentiation between STAS and artifact and floaters.[2, 14] A representative block was selected from each case, for the WSI based 3D analysis.

B. Sectioning and staining: The resected tissues were fixed in 10% buffered formalin and processed as the standard protocol. The tissues were embedded in medium melting point 56°C. The selected formalin-fixed, paraffin-embedded (FFPE) blocks were retrieved from the archive of the department of Pathology, MSKCC.

Each selected FFPE block was re-embedded into a new paraffin block and sectioned into 350 serial sections, 5 μm each using the AS-410 Automated Tissue Sectioning System (Dainippon Seki, Kyoto, Japan). The first 100 sections were stained by H&E. The next 200

sections were stained by double IHC staining and the last 50 sections were stained by IF using the multiplex IF panel. The stains are discussed in detail in the next section. The three cases of MIP STAS were stained using H&E, IHC and IF stains. The SN case was evaluated by H&E as well as IHC double IHC staining for TTF-1 and CD31 in addition to E-cadherin and type IV collagen stains.

C. Multiplex Immunofluorescence (IF) stains: The protocol for the multiplex IF was optimized in collaboration with the MSKCC Pathology Imaging Lab and Molecular Cytology Core Facility. Multiplex IF experiments were done using the following four antibodies: Collagen type IV, TTF1, CD31 and E-Cadherin. The Supplementary Table 1 shows the detailed information of the primary and secondary antibodies.

In brief, preceding the application of the primary antibody, the tissue sections were incubated for 8 min with Endogenous Biotin Block from Ventana (Ref#760–050). The incubation of the slides with the primary antibodies was done for 3–5 hours. The biotinylated secondary antibody was applied for 60 minutes. The fluorescent detection was carried out with Streptavidin-HRP D (Ventana Medical Systems), followed by incubation with Tyramid-Alexa Fluors of various wavelengths (Invitrogen): Alexa-488 (#840953), −546 (#840954), −594 (#T20950) or 647 (#T40958).

To optimize the multiplex IF, important steps were followed: 1) a positive control with high level of expression for the targeted antigens, was used for the optimization of each antibody. 2) to avoid cross-talk between the antibodies and establish the optimal multiplex sequence, adjacent sections were stained separately with each of the four antibodies and establish the optimal multiplex sequence, adjacent sections were stained separately with each of the four antibodies and carefully inspected. The order of antibody detection used in the multiplex experiment was as follows: collagen type 4 (detected with Alexa 647), TTF-1 (Alexa 546), CD31 (Alexa 488) and E-Cadherin (Alexa 594).

TTF-1 stained the tumor cell nuclei, shown in yellow (Figure 4A&B). CD31 stained the endothelial cells in green. E-cadherin stained the tumor cell membranes shown in red and collagen type 4 stained basement membrane, shown in white.

D. IHC double-staining—IHC double staining was used to identify the relationship between tumor cells, blood vessels and collagen in the main tumor area and adjacent parenchyma or STAS area in the 3D images and to highlight the relationship between these cells and surrounding connective tissue in a 3D configuration. The IHC double staining was performed on 200 tissue sections of the three MIP STAS specimens. IHC staining was done using the same antibodies with the same clones used for the multiplex IF. Collagen IV/CD31 antibodies were double-stained together, and TTF-1/E-cadherin were stained together. The sections were stained using both IHC and multiplex IF in order to compare the results of IHC with those of IF, and to maintain the serial sectioning of the block. For visualization purpose, H&E and IHC double stains were performed alternatively, (i.e. slide 1: TTF1 and E-cadherin, slide 2: H&E, slide 3: CD31 and Type IV collagen). On the solid STAS case, IHC double staining for TTF-1 and CD31 was done on 5 serial unstained sections.

E. Digitizing and 3D reconstruction: The tissue sections slides were digitized to WSI by 20x (0.46–0.5 μm/ pixel resolution) using AperionAT2 (Leica Biosystems Inc, Buffalo Grove, IL, USA) and NanoZoomer 2.0HT (Hamamatsu Photonics, Hamamatsu, Shizuoka, Japan). IF stained slides were scanned by Panoramic FLASH III (3D Histech, Hungary) with 0.32 μm/ pixel resolution.

The 3D histology model was reconstructed from all image sets to analyze the structure and interrelation of STAS using the software Voloom (version 2.8.3–2.8.7, microDimensions GmbH, München, Germany). This software allows automatic stack montage with minimal intervention from the user except for image alignment, with capability of manual reconstruction. The 3D model of the best quality was selected for this study to ensure a high magnification enabling the best observation. 3D models were developed per stain group and combination of H&E and IHC. Imaris Imaging software version 8 (Bitplane, MA, US) was used for high magnification image analysis (cellular level of analysis) and visualization for both blight field and fluorescence stain.

F. Interpretation of staining: All H&E, IHC and IF stains were analyzed using the 3D images to identify STAS and to interpret its morphology and its relationship with the surrounding tissues. The 3D model was observed from low magnifications up to 20x which is the original WSI resolution. Three areas were arbitrarily defined for analysis in the final 3D model for detailed study: the first area includes the tumor; the second area includes the tumor and the adjacent lung parenchyma and the third one includes the lung parenchyma away from the tumor. (Supplementary figure 1 shows the workflow of the WSI based 3D reconstruction).

Results

Identification of the presence of STAS

The lung adenocarcinomas tumors reviewed were MIP predominant (N=3) and solid predominant (N=1). STAS was observed, by both 2D and 3D imaging, as tumor cells present within the air spaces, spreading in a continuous manner into the lung parenchyma beyond the edge of the main tumor.

In the three MIP predominant adenocarcinoma, STAS was present as MIP clusters (Figure 1). In the solid predominant adenocarcinoma, STAS was forming solid nests (Figure 2).

WSI based reconstruction of STAS: alveolar wall attachment

In the four adenocarcinoma specimens, by studying all the serial sections of the 3D reconstructed image of the whole FFPE block, STAS cells were seen attached to the alveolar walls of the lung parenchyma (Figures 1, 2, 3 and 4). The attachment of STAS to the alveolar walls was seen in the H&E stains (Figures 1, 2, 3 and 4) including the 3D reconstructions (Figure 3) and confirmed by the IHC and multiplex IF stains (Figures 5A and B). This observation was seen in both the MIP (Figure 1, 3, 4 and 5) and solid nest (Figure 2) pattern of STAS where focally there were attachments to the alveolar walls, with preservation of the alveolar wall septa. The attachment of STAS cells to the alveolar wall was similar both for areas near and far from the main tumor.

Multiplex IF and IHC Analysis: Relationship Between STAS and Alveolar Wall Vasculature

While WSI based 3D reconstruction using H&E slides demonstrated that STAS clusters focally attach to the alveolar wall and locate close to the alveolar wall vasculature (Figure 1C and 1D), the multiplex IF stains in combination with the 3D reconstruction enabled us to further evaluate the relationship between the tumor cells and the connective tissue of the underlying lung parenchyma (alveolar wall). These findings are consistent with the concept of blood vessel "co-option." (Figure 1, 3,4 and 5).

STAS MIP clusters and solid nests (TTF-1 positive) were well anchored to the alveolar walls and these attachments were highlighted by E-cadherin stain. In areas of STAS, tumor cells attached to the alveolar walls, focally replaced normal pneumocytes and were sometimes in very close proximity to the alveolar wall vasculature (Figure 4A–D, 5B and Supplementary Figure 2A). In the case of solid STAS, the tumor cell nests filling the alveolar spaces lacked CD31 positive blood vessels and they were closely opposed to the capillaries of the alveolar walls consistent with blood vessel co-option (Supplementary Figure 2A). E-cadherin showed positive cytoplasmic staining in all three MIP cases by IF and the single solid case by IHC both within STAS clusters (Figure 5A–C and Supplementary Figure 2C) and the main tumor (Supplementary Figure 2D, data not for the MIP main tumor not shown).

The alveolar walls in the area of attachment had preserved architecture: The CD31 positive endothelial cells highlighted the intra-alveolar septal vessels which were thin, oriented, without any new sprouts, and surrounded by a thin basement membrane (Collagen type 4 positive). The pneumocytes were normally present on the surface of the alveolar wall, except for the areas of attachment of STAS, where they were replaced by the malignant cells.

3D Morphological Findings of the MIP clusters

In the 2D images, STAS MIP clusters were found to have different morphologies such as florets, ring-like structures and large MIP clusters (Figures 1B–E, 2 and 4). The 3D imaging, allowed a better identification of the floret (Figure 3) and ring-like structures of the MIP clusters (Figures 3 Supplementary Figure 3, and Figure 6). The ring-like structures seen by 2D (Figure 1B–E) were "ball-like structures" by 3D (Figure 3 and 6). The malignant cells were arranged in the form of a sphere surrounding a central lumen. The MIP clusters, by 3D, were seen, in some areas, attached to each other, forming larger clusters or "fused" MIP clusters (Supplementary figure 2). These fused MIP clusters were seen connected to each other in the form of entangled rope and corresponded to large MIP clusters by 2D (Supplementary figure 3).

3-D Imaging, Immunohistochemistry and Multiplex IF of MIP Clusters in the Main Tumor

Within the main tumor by 3D imaging MIP clusters were also seen in the form of florets, ball-like structures and fused clusters. The finding that MIP clusters within the main tumor were structures lacking fibrovascular cores, was highlighted by the IHC and the IF 3D images. The MIP clusters showed lack of CD31 staining (Figure 4C), differentiating them from tangential cuts of the true papillary structures with their characteristic fibrovascular cores (positive CD31 staining). Similarly, in the solid adenocarcinoma, IHC for CD31

showed lack of CD31 positive blood vessels within the tumor cell nests both within the main tumor and the STAS clusters (Supplementary figure 2A and B).

Molecular Studies

Molecular studies using the next generation sequencing platform MSK IMPACT revealed that 1) one MIP STAS case had *EGFR* L858R and *TP53* mutations; 2) the solid STAS case had a *KRAS* G12A mutation and 3) in one tumor no mutations were detected in the clinically validated panel. The fourth case was only evaluated by fragment analysis and no mutations were found for *EGFR* exon 19, *EGFR* exon 20 and *ERBB2/HER2* exon 20 deletions on insertions.

Discussion

Our study, using WSI based 3D reconstruction with H&E, immunohistochemistry and multiplex IF stains, of lung adenocarcinomas expands upon the understanding of STAS biology. Although detached from the main tumor and appearing to be free floating in air spaces on 2-D H&E slides, our 3D studies demonstrated focal attachments of STAS cells to alveolar walls in a manner consistent with the concept known as “co-option” of the pre-existing blood vessels.[28–33] These findings suggest for the first time that tumor cells detach from the main tumor and migrate through air spaces to distant alveolar walls where they reattach through vessel co-option allowing them to survive and grow. This may explain the higher recurrence rate and worse survival for STAS positive tumors undergoing limited resection compared to lobectomy.[9–11, 34, 35] In addition, by 3D evaluation, the ring like structures that are known to occur both within the main tumor and in STAS clusters with the MIP pattern are actually spherical structures with a single layer of tumor cells surrounding an empty space. Also, clusters and nests of STAS cells were found to be attached to each other. Another interesting finding was the lack of endothelial cells in MIP and solid areas of the main tumors in addition to areas of MIP and solid STAS tumor cell clusters as confirmed by lack of CD31 staining consistent with the concept of the non-angiogenic pattern of lung cancer described over 20 years ago that was also explained by vessel co-option.[36–39]

STAS is a phenomenon of tumor spread that is unique to the lung which unlike any other organ system has alveolar spaces through which tumor cells can move. In other organs tumor invasion and metastatic spread occurs by direct invasion into adjacent tissues or through blood vessels or lymphatics. It is well recognized for cancer in general that the metastatic process involves tumor cell detachment from the main tumor and locomotion to distant locations where the tumor cells reattach and begin to grow.[40–43] For example, when a lung cancer metastasizes to the brain the tumor cells invade through the blood vessel wall, gain access to the circulating blood, migrate through the bloodstream and then reattach to the endothelium of the blood vessels in the brain and then invade through the blood vessel wall into the surrounding brain tissue.[40–43] Although this process often referred to as “seed and soil”, it is complex and highly dependent on multiple factors that including detachment of the tumor cells from the main tumor, a receptive local microenvironment for reattachment and tumor cell properties including epithelial-to mesenchymal transition (EMT) and various genetic characteristics that lead to reattachment and growth in the distant location. Based

upon our morphological observations in this study and the large body of published clinical data we hypothesize that a similar process is occurring in the lung with STAS. Discohesive tumor cells detach from the main tumor and migrate through the air spaces beyond the tumor edge and then reattach to alveolar walls, leading to intrapulmonary spread. In the blood stream the number of circulating tumor cells is known to far exceed the number of overt distant metastatic foci that develop.[40] Similarly we suspect that in the lung, the number of STAS cells spreading through the air spaces far exceeds the number that actually reattach and form intrapulmonary metastatic deposits.

Concern has been expressed about how the airspace tumor cells of STAS can survive. It is well known that cells such as macrophages and lymphocytes can survive within alveolar spaces. So similarly, STAS tumor cells may remain viable as they migrate within airspaces to intraparenchymal sites distant from the main tumor where they reattach to alveolar walls through vessel co-option. In this study our 3D analyses have shown that focally some tumor cells of STAS are attached to alveolar walls and are not free floating in the air spaces as they appear in two dimensional routine histologic sections. These attachments appear to occur in association with the mechanism of vessel co-option. We propose that discohesive tumor cells become detached from the main tumor and migrate into the surrounding lung parenchyma through the air spaces in the form of STAS. Then some of these STAS clusters attach to alveolar walls and through vascular co-option they gain access to the alveolar vasculature allowing them to grow and form tumor implants in the lung parenchyma surrounding the tumor. However, similar to circulating tumor cells in the blood stream, the number of tumor cells spreading through the air spaces likely far exceeds the number that form microscopic alveolar wall attachments distant to the main tumor. This corresponds to our observation that the attachments of STAS cells to the alveolar walls are focal and not seen with all STAS cells.

Although the definition of MIP adenocarcinoma states that the tumor cell clusters lack fibrovascular cores, our findings of the lack of blood vessels both within the main tumor of three MIP and one solid adenocarcinomas as well as in both MIP and solid STAS tumor cell clusters has significant implications. These observations are consistent with the concept of the non-angiogenic pattern of lung cancer and blood vessel co-option that has been recognized for over 20 years.[37–39] Blood vessel co-option is essentially how tumors hijack preexisting vascular environments to thrive.[18, 19, 21, 28, 31, 32] Our finding of blood vessel co-option in re-attached STAS clusters explains how these tumor cells continue to survive and grow in the lung parenchyma beyond the tumor edge. It also can be compared to the concept of non-angiogenic lung cancer where vascular co-option has been a fundamental explanation for how tumor cells grow without their own vasculature.[19, 38] Although the concepts of MIP adenocarcinoma and STAS with both MIP and solid patterns did not develop until many years after the concept of nonangiogenic lung cancers was generated, the description of the alveolar pattern of nonsmall cell carcinoma corresponding to the non-angiogenic type of lung cancer may have included cases of what we now call MIP adenocarcinoma and possibly some cases of what we now call STAS.[36, 38] Similar to MIP and solid adenocarcinoma as well as STAS the nonangiogenic pattern of lung cancer was associated with poor prognosis.[38] The concept of nonangiogenic cancers has also been suggested to have therapeutic implications as a potential mechanism of resistance to anti-angiogenesis

therapy such as bevacizumab[31, 33] and as a possible biomarker for immunomodulatory therapy.[33] Whether the finding of STAS as a non-angiogenic form of lung cancer spread can have therapeutic implications needs to be investigated.

In our study, the attachment of STAS cells to the lung alveolar wall and STAS blood vessel co-option phenomenon was consistent and similar for both areas near and far from the main tumor, which gives a clue to explain how these cells could survive in adjacent lung parenchyma regardless of their position from the main tumor. It also provides an explanation why multiple studies have shown that the recurrence free survival and overall survival is significantly worse in patients who undergo limited resection compared to lobectomy.[1–4, 9, 11, 34, 44] Based on our findings in this 3D and multiplex immunohistochemical study, we hypothesize that in patients with limited resection and STAS who recur, that some of the STAS cells may have migrated beyond the limited resection margin and reattached by vessel co-option, allowing them to grow and leading to the recurrence.

One of the most interesting findings using the combined 3D reconstruction technology and the different stains was the STAS MIP cluster morphology. MIP clusters were either in the form of florets, ball-like or fused form where the clusters are attached to each other. The ball-like structure, a complete sphere consisting of a single layer of malignant cells surrounding an empty lumen, explains the ring-form seen in the 2D slides. The difference in morphology between 2D and 3D images was due to the different sectioning plane of the cut in the 2D slides sections. These ring-like structures were previously recognized in the 2011 IASLC/ATS/ERS lung adenocarcinoma classification and the 2015 WHO Classification,[13, 45] however what role they play in tumor behavior is not known. Given the ability of balls to roll and move along surfaces it is possible these rings or spheres represent structures that facilitate spread through air spaces. The formation of these spheres is similar to the structures described as “spheroids” that are seen in cell cultures of multiple types of cancers including lung cancers.[46–48] So the ability of these MIP tumor cells to grow as spheres within airspaces may be due either to similarities to the microenvironment seen in cell cultures and/or some inherent properties of the tumor cell surfaces that allow them to adhere to each other in these spherical structures. Interestingly 3D tumor spheroids have been suggested as in vitro models to mimic in vivo human solid tumors resistance to therapeutic drugs.[48]

The current study represents the first study of STAS utilizing 3D technology in combination with H&E, immunohistochemical and multiplex immunoflourescence stains. It shows the morphology, the cellular and protein interactions in the main tumor, as well as the adjacent lung parenchyma where STAS was present. The 3D image reconstruction of tumor specimens provided a geographical mapping of the tumor and its microenvironment, with accurate details of the tissue specimen. The additional IHC and multiplex IF stains permitted the detection of multiple antigens expression at the same time. The combination of 3D with H&E, IHC, and IF stains, allowed for the detection of the cellular and proteins interactions, which allowed for novel morphologic observations that have provided valuable insights into the morphological and biological significance of STAS.[22, 23]

The limitation of this study includes a small cohort, which will be expanded in the future studies of STAS in lung adenocarcinoma as well as other lung cancer subtypes with the use of more 3D imaging and multiplex IF panels for a better understanding of the cellular and protein interactions between STAS and the adjacent lung parenchyma.

Conclusions:

Using WSI combined with 3D reconstruction imaging using H&E, immunohistochemical and multiplex immunofluorescence stains demonstrated that although detached from the main tumor and appearing to be free floating in air spaces in 2-D, we demonstrated focal attachments of STAS cells to alveolar walls in a manner consistent with the concept known as “co-option” of the pre-existing blood vessels. Thus, our 3D studies provide morphologic evidence for the first time suggesting that tumor cells detach from the main tumor and migrate through air spaces to distant alveolar walls where they reattach through vessel co-option. In addition, by 3D evaluation, the ring like structures that are known to occur both within the main tumor and in STAS clusters with the MIP pattern are spherical structures with a single layer of tumor cells surrounding an empty space. In addition, the lack of endothelial cells in micropapillary and solid areas of the main tumor as well as within MIP and solid STAS clusters as confirmed by lack of CD31 staining is consistent with the concept of the non-angiogenic pattern of lung cancer. The ability of STAS cells to reattach to alveolar walls through vessel co-option after migrating away from the main tumor may be an explanation for the higher rates of recurrence and worse survival for patients with STAS who undergo limited resection rather than lobectomy.

Supplementary Material

Refer to Web version on PubMed Central for supplementary material.

Abbreviations:

AS	Auto slide
D	dimensional
FFPE	Formalin-fixed paraffin-embedded
H&E	hematoxylin and eosin
IF	immunofluorescence
IHC	immunohistochemistry
MIP	micropapillary
SNP	solid nest STAS
SCC	squamous cell carcinoma
STAS	spread through air spaces

WHO	World Health Organization
WSI	whole slide imaging

REFERENCES

1. Warth A, Muley T, Kossakowski CA, Goeppert B, Schirmacher P, Dienemann H, Weichert W. Prognostic Impact of Intra-alveolar Tumor Spread in Pulmonary Adenocarcinoma. The American journal of surgical pathology 2015;39:793–801. [PubMed: 25723114]
2. Kadota K, Nitadori J, Sima CS, Ujiie H, Rizk NP, Jones DR, Adusumilli PS, Travis WD. Tumor Spread through Air Spaces is an Important Pattern of Invasion and Impacts the Frequency and Location of Recurrences after Limited Resection for Small Stage I Lung Adenocarcinomas. J Thorac Oncol 2015;10:806–14. [PubMed: 25629637]
3. Shiono S, Yanagawa N. Spread through air spaces is a predictive factor of recurrence and a prognostic factor in stage I lung adenocarcinoma. Interact Cardiovasc Thorac Surg 2016;23:567–72. [PubMed: 27354463]
4. Dai C, Xie H, Su H, She Y, Zhu E, Fan Z, Zhou F, Ren Y, Xie D, Zheng H, Kadeer X, Chen D, Zhang L, Jiang G, Wu C, Chen C. Tumor Spread through Air Spaces Affects the Recurrence and Overall Survival in Patients with Lung Adenocarcinoma >2 to 3 cm. J Thorac Oncol 2017;12:1052–60. [PubMed: 28389373]
5. Sun PL, Liu JN, Cao LQ, Yao M, Gao HW. [To evaluate the clinicopathologic characteristics and outcome of tumor cells spreading through air spaces in patients with adenocarcinoma of lung]. Zhonghua bing li xue za zhi = Chinese journal of pathology 2017;46:303–8. [PubMed: 28468034]
6. Uruga H, Fujii T, Fujimori S, Kohno T, Kishi K. Semiquantitative Assessment of Tumor Spread through Air Spaces (STAS) in Early-Stage Lung Adenocarcinomas. J Thorac Oncol 2017;12:1046–51. [PubMed: 28363628]
7. Toyokawa G, Yamada Y, Tagawa T, Kozuma Y, Matsubara T, Haratake N, Takamori S, Akamine T, Oda Y, Maehara Y. Significance of Spread Through Air Spaces in Resected Pathological Stage I Lung Adenocarcinoma. Ann Thorac Surg 2018;105:1655–63. [PubMed: 29453963]
8. Yi E, Bae MK, Cho S, Chung JH, Jheon S, Kim K. Pathological prognostic factors of recurrence in early stage lung adenocarcinoma. ANZ journal of surgery 2018;88:327–31. [PubMed: 28702948]
9. Eguchi T, Kameda K, Lu S, Bott MJ, Tan KS, Montecalvo J, Chang JC, Rekhtman N, Jones DR, Travis WD, Adusumilli PS. Lobectomy Is Associated with Better Outcomes than Sublobar Resection in Spread through Air Spaces (STAS)-Positive T1 Lung Adenocarcinoma: A Propensity Score-Matched Analysis. J Thorac Oncol 2019;14:87–98. [PubMed: 30244070]
10. Kadota K, Kushida Y, Kagawa S, Ishikawa R, Ibuki E, Inoue K, Go T, Yokomise H, Ishii T, Kadowaki N, Haba R. Limited Resection Is Associated With a Higher Risk of Locoregional Recurrence than Lobectomy in Stage I Lung Adenocarcinoma With Tumor Spread Through Air Spaces. The American journal of surgical pathology 2019;43:1033–41. [PubMed: 31107717]
11. Liu H, Yin Q, Yang G, Qie P. Prognostic Impact of Tumor Spread Through Air Spaces in Non-small Cell Lung Cancers: a Meta-Analysis Including 3564 Patients. Pathol Oncol Res 2019.
12. Terada Y, Takahashi T, Morita S, Kashiwabara K, Nagayama K, Nitadori JI, Anraku M, Sato M, Shinozaki-Ushiku A, Nakajima J. Spread through air spaces is an independent predictor of recurrence in stage III (N2) lung adenocarcinoma. Interact Cardiovasc Thorac Surg 2019.
13. Travis WD, Brambilla E, Burke AP, Marx A, Nicholson AG. WHO Classification of Tumours of the Lung, Pleura, Thymus and Heart. 4th ed. Lyon: International Agency for Research on Cancer; 2015.
14. Lu S, Tan KS, Kadota K, Eguchi T, Bains S, Rekhtman N, Adusumilli PS, Travis WD. Spread through Air Spaces (STAS) Is an Independent Predictor of Recurrence and Lung Cancer-Specific Death in Squamous Cell Carcinoma. J Thorac Oncol 2017;12:223–34. [PubMed: 27693541]
15. Kadota K, Kushida Y, Katsuki N, Ishikawa R, Ibuki E, Motoyama M, Nii K, Yokomise H, Bandoh S, Haba R. Tumor Spread Through Air Spaces Is an Independent Predictor of Recurrence-free Survival in Patients With Resected Lung Squamous Cell Carcinoma. The American journal of surgical pathology 2017;41:1077–86. [PubMed: 28498282]

16. Aly RG, Rekhtman N, Li X, Takahashi Y, Eguchi T, Tan KS, Rudin CM, Adusumilli PS, Travis WD. Spread Through Air Spaces (STAS) Is Prognostic in Atypical Carcinoid, Large Cell Neuroendocrine Carcinoma, and Small Cell Carcinoma of the Lung. J Thorac Oncol 2019;14:1583–93. [PubMed: 31121325]
17. Yokoyama S, Murakami T, Tao H, Onoda H, Hara A, Miyazaki R, Furukawa M, Hayashi M, Inokawa H, Okabe K, Akagi Y. Tumor Spread Through Air Spaces Identifies a Distinct Subgroup With Poor Prognosis in Surgically Resected Lung Pleomorphic Carcinoma. Chest 2018;154:838–47. [PubMed: 29932891]
18. Kaessmeyer S, Bhoola K, Baltic S, Thompson P, Plendl J. Lung cancer neovascularisation: Cellular and molecular interaction between endothelial and lung cancer cells. Immunobiology 2014;219:308–14. [PubMed: 24355365]
19. Pezzella F, Gatter K. Non-angiogenic tumours unveil a new chapter in cancer biology. J Pathol 2015;235:381–3. [PubMed: 25351454]
20. Qian CN. Hijacking the vasculature in ccRCC--co-option, remodelling and angiogenesis. Nature reviews Urology 2013;10:300–4. [PubMed: 23459032]
21. Zhao C, Yang H, Shi H, Wang X, Chen X, Yuan Y, Lin S, Wei Y. Distinct contributions of angiogenesis and vascular co-option during the initiation of primary microtumors and micrometastases. Carcinogenesis 2011;32:1143–50. [PubMed: 21515914]
22. Hashimoto N, Bautista PA, Haneishi H, Snuderl M, Yagi Y. Development of a 2D Image Reconstruction and Viewing System for Histological Images from Multiple Tissue Blocks: Towards High-Resolution Whole-Organ 3D Histological Images. Pathobiology 2016;83:127–39. [PubMed: 27100217]
23. Fujisawa S, Yarilin D, Fan N, Turkekul M, Xu K, Barlas A, Manova-Todorova K. Understanding the three-dimensional world from two-dimensional immunofluorescent adjacent sections. Journal of pathology informatics 2015;6:27. [PubMed: 26110094]
24. Handschuh S, Schwaha T, Metscher BD. Showing their true colors: a practical approach to volume rendering from serial sections. BMC developmental biology 2010;10:41. [PubMed: 20409315]
25. Streicher J, Weninger WJ, Muller GB. External marker-based automatic congruencing: a new method of 3D reconstruction from serial sections. The Anatomical record 1997;248:583–602. [PubMed: 9268147]
26. Onozato ML, Klepeis VE, Yagi Y, Mino-Kenudson M. A role of three-dimensional (3D)-reconstruction in the classification of lung adenocarcinoma. Anal Cell Pathol (Amst) 2012;35:79–84. [PubMed: 21955723]
27. Onozato ML, Kovach AE, Yeap BY, Morales-Oyarvide V, Klepeis VE, Tammireddy S, Heist RS, Mark EJ, Dias-Santagata D, Iafrate AJ, Yagi Y, Mino-Kenudson M. Tumor islands in resected early-stage lung adenocarcinomas are associated with unique clinicopathologic and molecular characteristics and worse prognosis. The American journal of surgical pathology 2013;37:287–94. [PubMed: 23095504]
28. Szabo V, Bugyik E, Dezso K, Ecker N, Nagy P, Timar J, Tovari J, Laszlo V, Bridgeman VL, Wan E, Frentzas S, Vermeulen PB, Reynolds AR, Dome B, Paku S. Mechanism of tumour vascularization in experimental lung metastases. J Pathol 2015;235:384–96. [PubMed: 25319725]
29. Pinto MP, Sotomayor P, Carrasco-Avino G, Corvalan AH, Owen GI. Escaping Antiangiogenic Therapy: Strategies Employed by Cancer Cells. International journal of molecular sciences 2016;17.
30. Qian CN, Tan MH, Yang JP, Cao Y. Revisiting tumor angiogenesis: vessel co-option, vessel remodeling, and cancer cell-derived vasculature formation. Chin J Cancer 2016;35:10. [PubMed: 26747273]
31. Bridgeman VL, Vermeulen PB, Foo S, Bilecz A, Daley F, Kostaras E, Nathan MR, Wan E, Frentzas S, Schweiger T, Hegedus B, Hoetzenecker K, Renyi-Vamos F, Kuczynski EA, Vasudev NS, Larkin J, Gore M, Dvorak HF, Paku S, Kerbel RS, Dome B, Reynolds AR. Vessel co-option is common in human lung metastases and mediates resistance to anti-angiogenic therapy in preclinical lung metastasis models. J Pathol 2017;241:362–74. [PubMed: 27859259]
32. Winkler F Hostile takeover: how tumours hijack pre-existing vascular environments to thrive. J Pathol 2017;242:267–72. [PubMed: 28390068]

33. van Dam PJ, Daelemans S, Ross E, Waumans Y, Van Laere S, Latacz E, Van Steen R, De Pooter C, Kockx M, Dirix L, Vermeulen PB. Histopathological growth patterns as a candidate biomarker for immunomodulatory therapy. Seminars in cancer biology 2018;52:86–93. [PubMed: 29355613]
34. Bains S, Eguchi T, Warth A, Yeh YC, Nitadori JI, Woo KM, Chou TY, Dienemann H, Muley T, Nakajima J, Shinozaki-Ushiku A, Wu YC, Lu S, Kadota K, Jones DR, Travis WD, Tan KS, Adusumilli PS. Procedure-Specific Risk Prediction for Recurrence in Patients Undergoing Lobectomy or Sublobar Resection for Small (</=2 cm) Lung Adenocarcinoma: An International Cohort Analysis. J Thorac Oncol 2019;14:72–86. [PubMed: 30253972]
35. Shiono S, Endo M, Suzuki K, Yarimizu K, Hayasaka K, Yanagawa N. Spread Through Air Spaces Is a Prognostic Factor in Sublobar Resection of Non-Small Cell Lung Cancer. Ann Thorac Surg 2018;106:354–60. [PubMed: 29625101]
36. Pezzella F, Pastorino U, Tagliabue E, Andreola S, Sozzi G, Gasparini G, Menard S, Gatter KC, Harris AL, Fox S, Buyse M, Pilotti S, Pierotti M, Rilke F. Non-small-cell lung carcinoma tumor growth without morphological evidence of neo-angiogenesis. AmJPathol 1997;151:1417–23.
37. Passalidou E, Trivella M, Singh N, Ferguson M, Hu J, Cesario A, Granone P, Nicholson AG, Goldstraw P, Ratcliffe C, Tetlow M, Leigh I, Harris AL, Gatter KC, Pezzella F. Vascular phenotype in angiogenic and non-angiogenic lung non-small cell carcinomas. BrJCancer 2002;86:244–9.
38. Sardari NP, Colpaert C, Blyweert B, Kui B, Vermeulen P, Ferguson M, Hendriks J, Weyler J, Pezzella F, Van ME, Van SP. Prognostic value of nonangiogenic and angiogenic growth patterns in non-small-cell lung cancer. BrJCancer 2004;91:1293–300.
39. Sardari Nia P, Van Marck E, Weyler J, Van Schil P. Prognostic value of a biologic classification of non-small-cell lung cancer into the growth patterns along with other clinical, pathological and immunohistochemical factors. European journal of cardio-thoracic surgery: official journal of the European Association for Cardio-thoracic Surgery 2010;38:628–36. [PubMed: 20452237]
40. Massague J, Obenauf AC. Metastatic colonization by circulating tumour cells. Nature 2016;529:298–306. [PubMed: 26791720]
41. Liu Q, Zhang H, Jiang X, Qian C, Liu Z, Luo D. Factors involved in cancer metastasis: a better understanding to “seed and soil” hypothesis. Mol Cancer 2017;16:176. [PubMed: 29197379]
42. Massague J, Batlle E, Gomis RR. Understanding the molecular mechanisms driving metastasis. Mol Oncol 2017;11:3–4. [PubMed: 28085221]
43. Akhtar M, Haider A, Rashid S, Al-Nabet A. Paget’s “Seed and Soil” Theory of Cancer Metastasis: An Idea Whose Time has Come. Adv Anat Pathol 2019;26:69–74. [PubMed: 30339548]
44. Morimoto J, Nakajima T, Suzuki H, Nagato K, Iwata T, Yoshida S, Fukuyo M, Ota S, Nakatani Y, Yoshino I. Impact of free tumor clusters on prognosis after resection of pulmonary adenocarcinoma. J Thorac Cardiovasc Surg 2016;152:64–72 e1. [PubMed: 27343907]
45. Travis WD, Brambilla E, Noguchi M, Geisinger KR, Beer D, Powell CA, Johnson B, Riely GJ, Rusch VW, Asamura H, Garg K, Austin J, Aberle D, Brambilla C, Flieder D, Franklin WA, Gazdar A, Gould MK, Hasleton P, Henderson D, Hirsch F, Huber RM, Ishikawa Y, Jett JR, Johnson D, Kerr K, Kuriyama K, Lee JS, Miller VA, Mitsudomi T, Nicholson AG, Petersen I, Roggli V, Rosell R, Saijo N, Sanchez-Cespedes M, Scagliotti G, Sculier JP, Takahashi T, Thunnissen FB, Tsao M, Tsuboi M, Van Schil PE, Vansteenkiste J, Wistuba I, Yankelevitz D, Yatabe Y, Yang PC. The New IASLC/ATS/ERS international multidisciplinary lung adenocarcinoma classification. JThoracic Oncol 2011;6:244–85.
46. Nakano T, Kanai Y, Amano Y, Yoshimoto T, Matsubara D, Shibano T, Tamura T, Oguni S, Katashiba S, Ito T, Murakami Y, Fukayama M, Murakami T, Endo S, Niki T. Establishment of highly metastatic KRAS mutant lung cancer cell sublines in long-term three-dimensional low attachment cultures. PLoS One 2017;12:e0181342. [PubMed: 28786996]
47. Tevis KM, Colson YL, Grinstaff MW. Embedded Spheroids as Models of the Cancer Microenvironment. Advanced biosystems 2017;1.
48. Nunes AS, Barros AS, Costa EC, Moreira AF, Correia IJ. 3D tumor spheroids as in vitro models to mimic in vivo human solid tumors resistance to therapeutic drugs. Biotechnology and bioengineering 2019;116:206–26. [PubMed: 30367820]

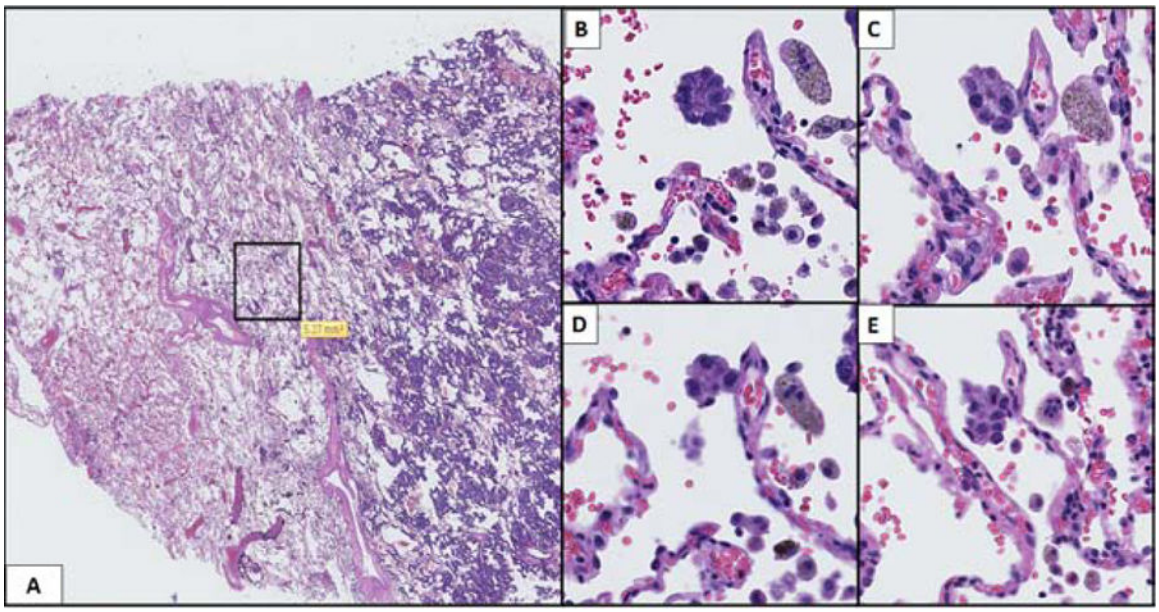

Figure 1.

STAS was present as MIP clusters. In in the 2D images, Numerous STAS MIP clusters were found in the alveolar parenchyma extend in a continuous manner within air spaces as far as 1.4 cm to the left of the image beyond the edge of the tumor (A). The 3D imaging (B-D) focused on the area highlighted in the black box in A, with serial sectioning demonstrated how the same floret micropapillary cluster that appeared floating in the air space in B, is attached to the alveolar wall on deeper sections C, D and E.

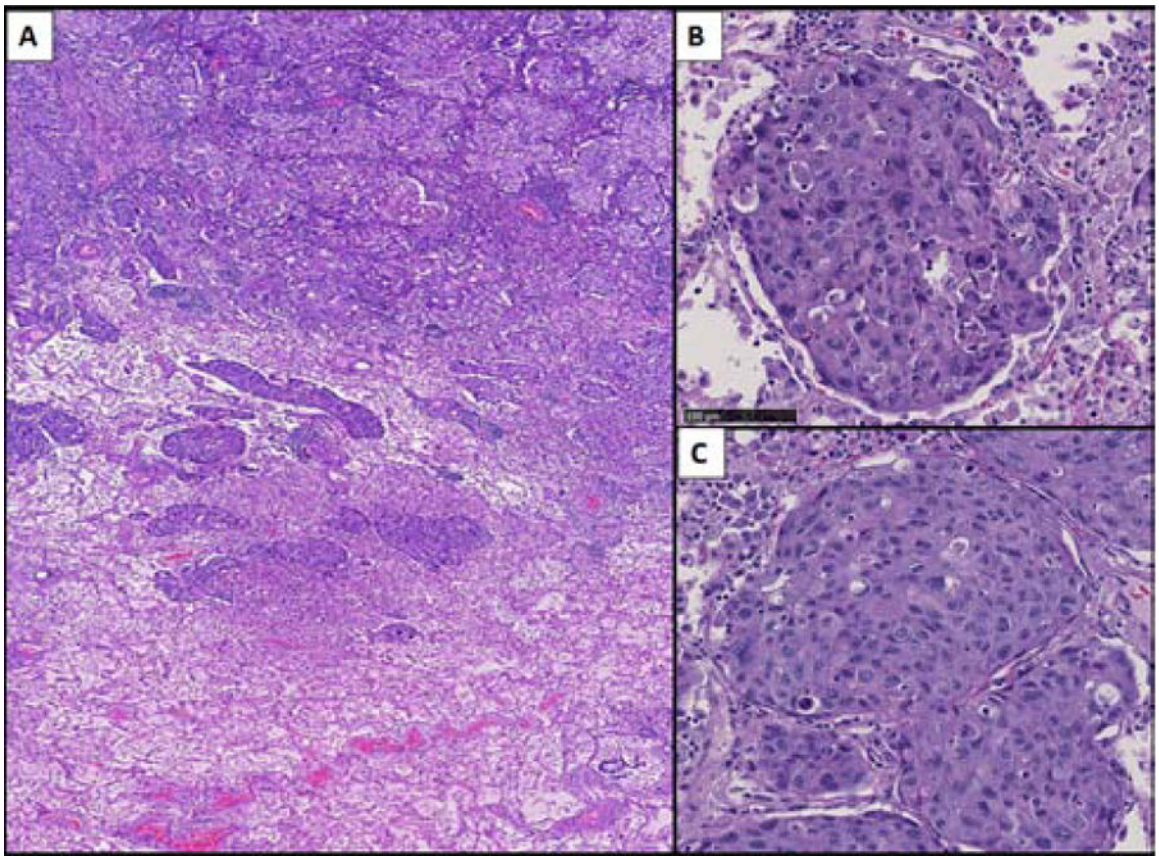

Figure 2.

STAS in this case formed solid nests. A) Solid predominant adenocarcinoma with solid nests of STAS extending beyond the edge of the tumor (marked in blue line) into surrounding air spaces (H&E). B) The STAS solid nests fill the alveolar space and are seen attached to the alveolar wall (black arrows), replacing the normal pneumocytes. C) The STAS solid nests are seen at one serial section attached to the alveolar wall (black arrow) (C) (H&E, original magnification x20)

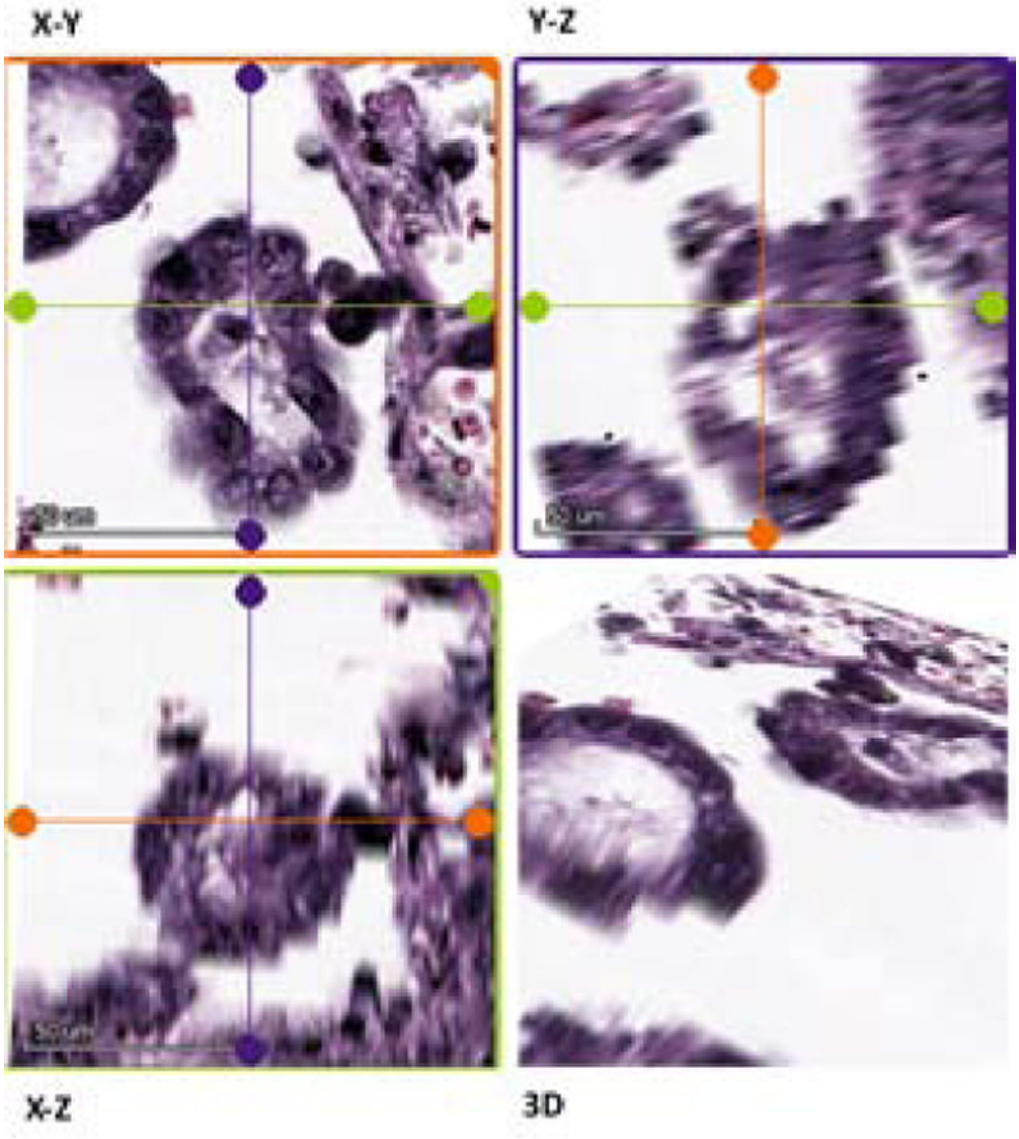

Figure 3:

3D visualization of ATTACHED STAS CLUSTER. 3D window (bottom right) shows reconstructed 3D structure of ring-like STAS cluster with corresponding view of the other 3 windows. X-Y shows same plane with a H&E slide of corresponding slide with green line on Y-Z and Blue line on X-Z. Ring like structures are seen in 3D.

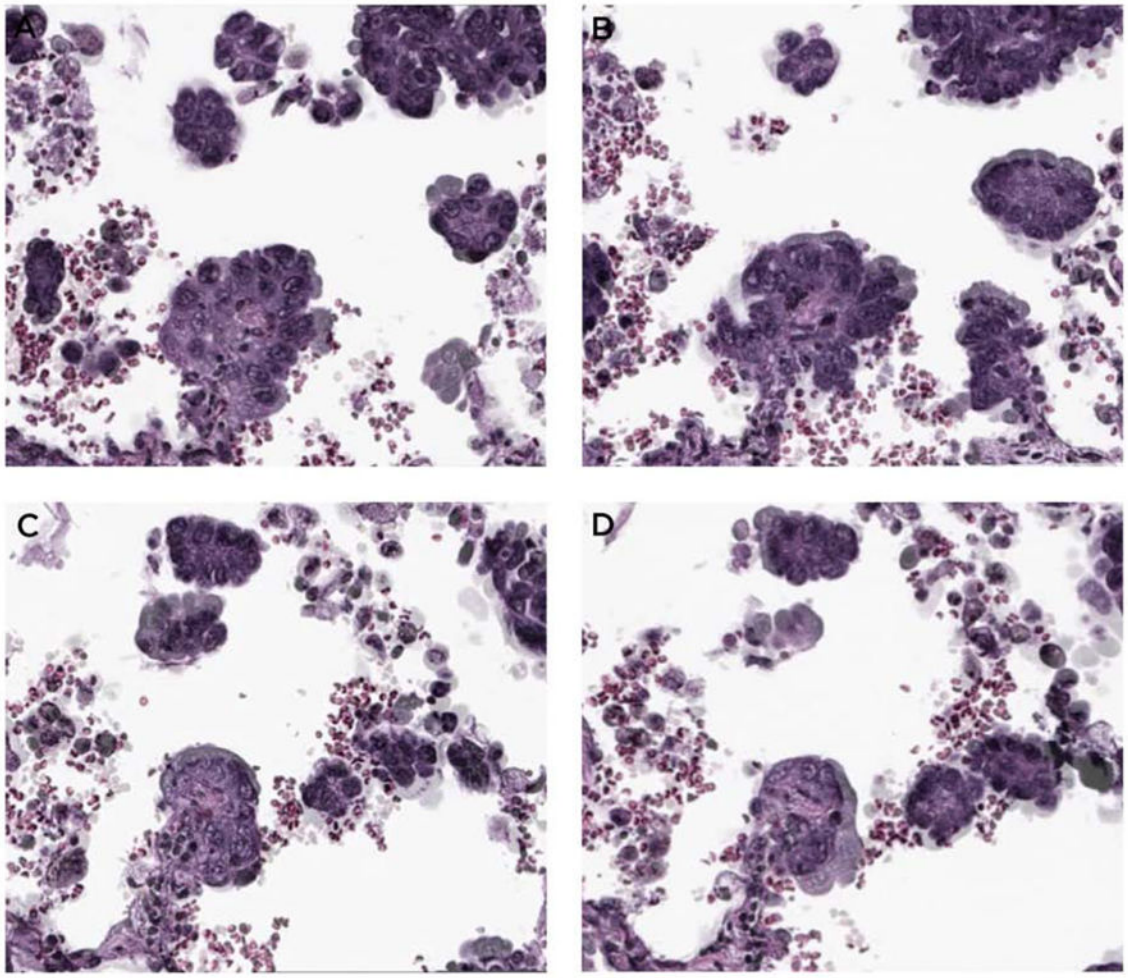

Figure 4:
Attachment of STAS MIP clusters to alveolar wall. In these serial H&E sections in a STAS area away from the main tumor, in addition to STAS MIP clusters that appear to be floating in the air spaces, there is a direct attachment to the alveolar wall (A-D, arrows).

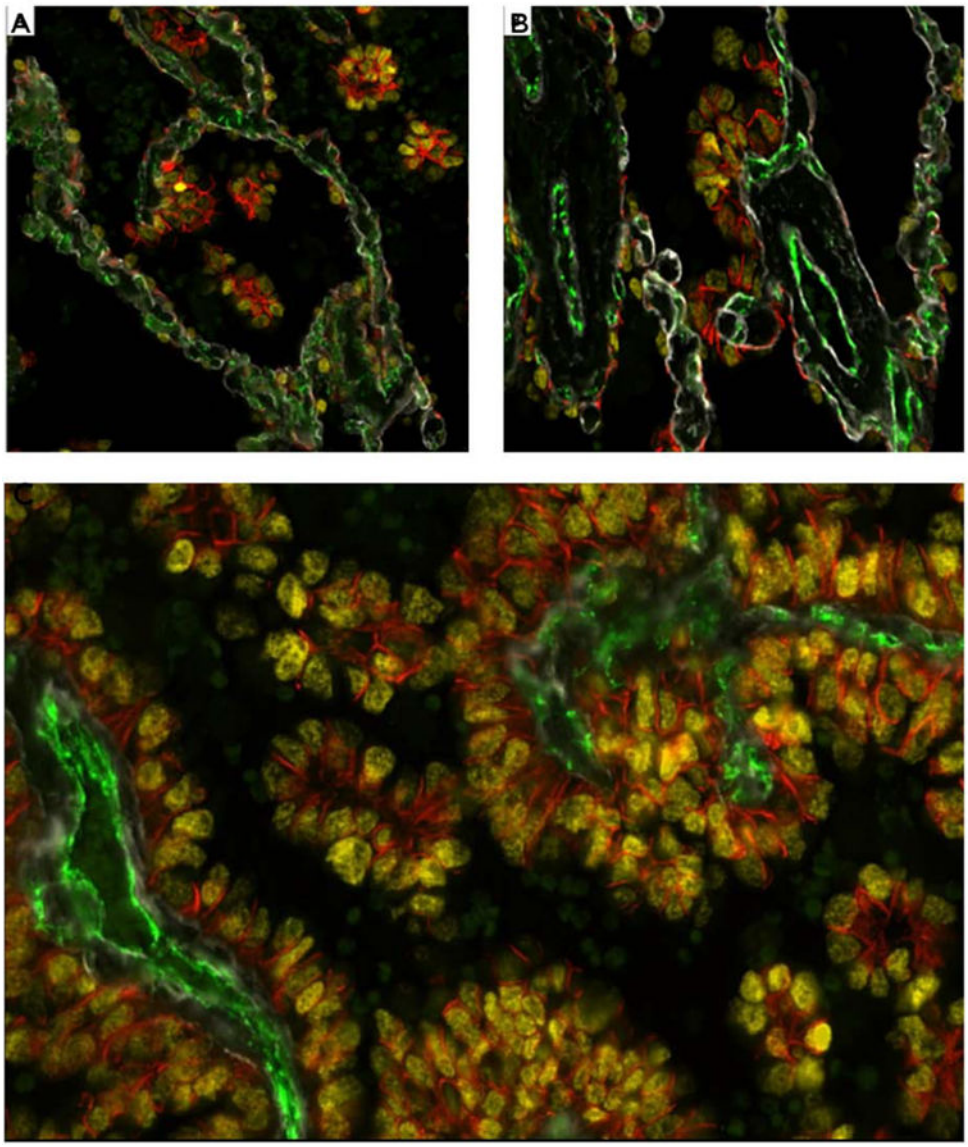

Figure 5: Immunofluorescence (IF) staining:

(A and B) IF stain from an area of lung parenchyma beyond the edge of the tumor (STAS area) shows the nuclear yellow TTF1 staining of the micropapillary (MIP) STAS cells with attachments to the alveolar walls often in areas where the tumor cell cytoplasm is expressing membranous orange staining by E-cadherin (Figure 5A and B). The STAS cells focally are in close apposition to the pre-existing capillaries in the alveolar septa (CD31 positive, green). The alveolar walls show preserved architecture with thin regular capillaries with areas showing preserved type IV collagen of the alveolar wall basement membrane (Collagen IV, white). No endothelial cells or CD31 staining are seen within the STAS clusters. C: IF stain at one level of the main tumor shows the micropapillary (MIP) floret clusters adjacent to papillary structures of the main tumor. The section shows the MIP clusters attached to each other and attached to the papillary structures. The MIP clusters within the air spaces show no CD31 expression indicating lack of a central endothelial lined

vascular core (CD31 green negative), differentiating the MIP clusters from the tangential cut of papillary structures.

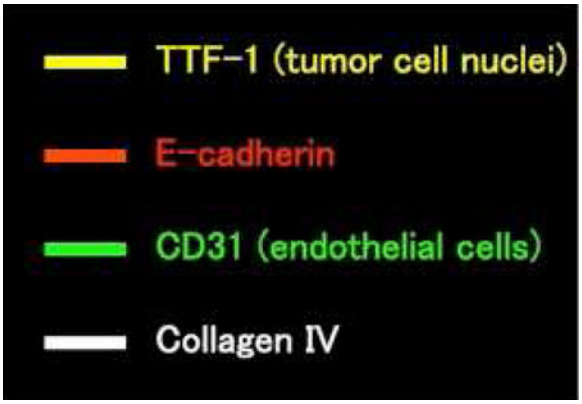

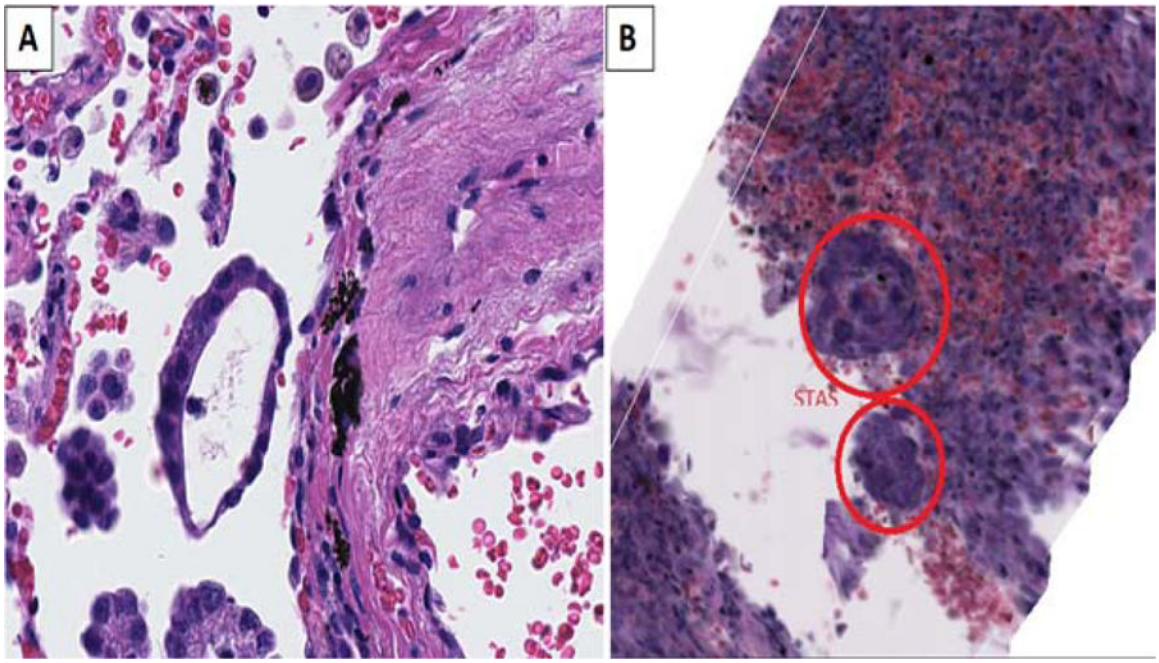

Figure 6:

A) Micropapillary (MIP) STAS appears as a ring-like structure in 2D. (B) however it is seen as a ball-like structure in 3D formed of malignant cells forming a sphere with a wall consisting of a single layer of tumor cells with a central empty lumen (H&E, original magnification x20)